Journal of Holography Applications in Physics
Volume 6, Issue 3, Summer 2026, 52–71
©Available online at http://jhap.du.ac.ir
DOI: 10.22128/jhap.2025.3149.1163
Online ISSN: 2783–3518

Regular article

Casimir Energy Traversable Wormholes in Symmetric Teleparallel Gravity

Sadhana[1] · Shweta[2] · Ambuj Kumar Mishra[3]

[1] Department of Mathematics, Institute of Applied Sciences and Humanities, GLA University, Mathura-281 406, Uttar Pradesh, India;
E-mail: sadhanasingh1305@gmail.com

[2] Department of Mathematics, Institute of Applied Sciences and Humanities, GLA University, Mathura-281 406, Uttar Pradesh, India;
E-mail: shwetaibs84@gmail.com

[3] Department of Mathematics, Institute of Applied Sciences and Humanities, GLA University, Mathura-281 406, Uttar Pradesh, India;
Corresponding Author E-mail: ambuj_math@rediffmail.com

Received: November 16, 2025; **Revised:** December 13, 2025; **Accepted:** December 29, 2025

Abstract. In recent years, research has concentrated on finding techniques to create traversable wormholes that circumvent the exotic matter problem or violate the null energy condition (NEC). Scientists are investigating alternate gravity theories and specific frameworks of ordinary matter that might potentially stabilize a wormhole throat, eliminating the necessity for negative energy density. Casimir energy, a quantum field theory phenomenon, provides a plausible option for producing traversable wormholes. Because Casimir energy can naturally produce specific regions of negative energy density, researchers are exploring how this artificial negative energy may function as the exotic matter needed to stabilize a wormhole's throat, potentially avoiding the need for theorized exotic matter. This research studies traversable wormhole geometries using Casimir energy as the source of the requisite exotic matter, looking at solutions within the framework of three different functional forms of $f(Q)$ gravity. The three functional forms taken are the power-law form, the inverse power-law form, and the logarithmic form for investigation. In all three cases, energy conditions are discussed. The anisotropy parameter and EoS parameter are analyzed to find a plausible solution for a traversable wormhole space-time.

Keywords: Wormholes; ECs; $f(Q)$ Gravity; Casimir Energy.

Contents

1 Introduction

We are not wrong if we say that some of the most creative and significant scientific theories were created by Einstein. Einstein's general theory of relativity (GR) has proven extremely successful at describing and predicting a wide range of phenomena. With technological advancements, methods like gravitational lensing, VIRGO, and EHT have experimentally proved it to be the majority correct theory of gravity [1–4]. Not a long while ago, gravity was assumed to be a force. In September 2015, the Advanced LIGO detector made the first-ever direct observation of gravitational waves, which are distortions in the curvature of spacetime. These particular waves were created by a black hole merger [5]. This validates one more prediction of GR.

The GR is defined by the solution of field equations, which further enables us to answer other physical phenomena like black holes, planetary dynamics, the evolution of the universe, etc. Among the numerous fascinating predictions of GR, physicists are particularly interested in the exciting theoretical prospect of traversable wormholes. Wormholes are imagined tunnel-shaped constructions having two entrances at either end joined by a throat. It generates a spacetime shortcut that connects two faraway locations. Wormholes remain essentially hypothetical, with no experimental evidence confirming their existence. However, interest in them is developing at a rapid pace, as they are regarded as potential portals for time travel and speedy interplanetary travel within realistic timelines.

Flamm first gave the idea of static wormholes connecting two asymptotically distant regions in space-time in the form of Schwarzschild solutions [6]. Traversable wormholes represent Einstein field equation solutions [7]. Einstein and Rosen suggested the Einstein-Rosen bridge, which expanded on the static wormhole idea, in 1935 [8]. Subsequently, similar solutions were discovered, including the Einstein-Rosen bridge, which links two regions of spacetime that are each described by a Schwarzschild solution [9,10]. Morris and Thorne introduced the idea of a spherically symmetric traversable wormhole, which was later shown to require exotic matter, and various models have explored how such wormholes could be supported by hypothetical fields like a tachyonic massless scalar field[11]. They, along with Yurtsever, put forward the idea of a time machine giving a probable traversable wormhole solution [12–16].

Currently, interest is growing in finding a solution for traversable WH with no event horizon or singularity, as the Schwarzschild metric fails to describe the spacetime geometry at the event horizon. To achieve this, the metric is adjusted, and constraints are enforced on the throat's properties via the implementation of the Birkhoff theorem [17], in which case the mass-energy is less than radial tension [18–21]. This leads to the violation of NEC and which in turn escorts the presence of phantom fluid or phantom energy. To eliminate this necessity of exotic matter in the wormhole geometry, several modified theories of gravity came into existence where the violation of the NEC is regarded as the effect of higher-order curvature terms. $f(R)$ gravity set the stage to achieve the thin shell traversable wormhole. $f(R,T)$ theory of gravity came into existence by coupling the geometry with matter terms, where for different forms of the function $f(R,T)$, wormhole solutions are explored [22–29].

Teleparallel gravity and various modified gravitational theories also find their way into the study of traversable wormholes [30–41]. Teleparallel theory [42,43] is one of the desirable alternatives to GR nowadays, which is examined for the possible solutions of wormhole geometries. In this theory, spacetime is curvature and torsion-free, with gravitational interactions described by the nonmetricity term Q. To evaluate these teleparallel gravity models, we express the $f(Q)$ gravity Lagrangian as an explicit function of redshift, which is represented by $f(z)$. This method can be justified using different observational tools, including data from quasars, the Cosmic Microwave Background, Baryon Acoustic Oscillations, and Gamma-Ray Bursts [44,45]. The different classes of gravitational modifications are introduced by various authors using the different functional forms of $f(Q)$, from which wormhole solutions and other cosmographical results are discussed [46–53].

As we have already discussed, the traversability of wormholes in GR is consequently obtained by the violation of NEC, which is unfortunately unavoidable in that case, as it indicates the existence of exotic matter as the threading matter in the wormhole throat, which possesses negative energy. Our motivation for the present paper derives from the above fact, as we try to develop solutions for traversable wormhole geometries, addressing the issue of negative energy by proposing that the negative energy required to keep the wormhole mouth open for the required duration can be obtained from a different energy source. Classical matter validates the NEC, and therefore, the derivation of wormholes is possible in the context of semi-classical gravity or quantum gravity. Casimir energy, the sole artificial method of producing negative energy at the moment, could be a promising source of the required exotic energy [54]. Casimir energy is generated in the vacuum created by two uncharged, parallel metallic plates positioned very close together. An attractive force arises from this event, a prediction made in 1948 and subsequently verified through experiments at Philips laboratories [55,56] and by other investigators more recently [57,58].

In the present article, we have discussed traversable WH solutions within the context of teleparallel gravity, inducing the Casimir energy system in three different expressions for $f(Q)$. In the first case, we try to explore the Casimir wormhole geometry, taking the power-law expression for $f(Q)$. The second and third cases are discussed using the inverse power law and logarithmic expression, respectively. The manuscript here is divided into six sections. The $f(Q)$ gravity is formed in Section 2. Section 3 discusses the fundamental criteria for the wormhole's shape function and offers the field equations inside the teleparallel gravity. Section 4 gives an insight into the required energy conditions. Casimir energy is further discussed in Section 5. In subsections of section 5, the WH solutions are examined for three different expressions for $f(Q)$. Section 6 presents the conclusions and remarks.

2 The Mechanism of Symmetric Teleparallel Gravity

In the present article we take the action for symmetric teleparallel gravity [59] as

$$S = \frac{1}{2} \int \left[f\left(Q\right) + 2\mathcal{L}_{\mu} \right] \sqrt{-g} d^4 x, \tag{2.1}$$

where, $\mathcal{L}_{\mu}$ is the matter Lagrangian density while the function $f(Q)$ is taken with regard to the non-metricity term Q, g gives determinant of the metric g_{lm}.

The non-metricity tensor is given by

$$Q_{\lambda lm} = \nabla_{\lambda lm}. \tag{2.2}$$

The non-metricity tensor asserts two independent traces as

$$Q_{\phi} = Q_{\phi}{}^{l}{}_{l} \qquad , \qquad \bar{Q}_{\phi} = Q^{l}{}_{\phi l}. \tag{2.3}$$

The non-metricity conjugate corresponding to super-potential of this new GR, as referred by Jiminez et.al. [43], is

$$P^{\phi}{}_{lm} = \frac{1}{4} \left[-Q^{\phi}{}_{lm} + 2Q^{\phi}{}_{lm} + Q^{\phi} g_{lm} - \bar{Q}^{\phi} g_{lm} - \delta^{\phi}_{l} \left(Q_m\right) \right]. \tag{2.4}$$

This is obtained by analyzing the form of the non-metricity tensor

$$Q = -Q_{\phi lm} P^{\phi lm}. \tag{2.5}$$

The energy momentum tensor describes the property of the matter spread in space-time, as given by

$$T_{lm} = -\frac{2}{\sqrt{-g}} \frac{\delta\left(\sqrt{-g}\mathcal{L}_{\mu}\right)}{\delta g^{lm}}. \tag{2.6}$$

The motion equations are obtained when we vary the action given in Eq. (2.1) with respect to the metric tensor g_{lm}, written as

$$\frac{2\nabla_{\eta}}{\sqrt{-g}}\left(\sqrt{-g} f_Q P^{\eta}{}_{lm}\right) + \frac{1}{2} g_{lm} f + f_Q \left(P_{l\eta\zeta} Q_m{}^{\eta\zeta} - 2Q_{\eta\zeta l} P^{\eta}{}_{\zeta m}\right) = -T_{lm}, \tag{2.7}$$

where total derivative of f with respect to Q is given by f_Q. On varying Eq. (2.1) with respect to the connections, we get the following relation

$$\nabla_l \nabla_m \left(\sqrt{-g} f_Q P^{\eta}{}_{lm}\right) = 0. \tag{2.8}$$

Consistent with the specified $f(Q)$ gravity, the field equations mandate the conservation of the energy-momentum tensor. This study is dedicated to detailing the gravitational field equations that dictate static and spherically symmetric solutions [60] for wormhole geometry.

3 Wormhole Structure and Solution of Field Equations in Symmetric Teleparallel Gravity

To represent the wormhole geometry, we consider the general static spherically symmetric line element of Morris-Thorne class

$$ds^2 = -\exp\left(2\phi(r)\right) dt^2 + \left(\frac{r - b\left(r\right)}{r}\right)^{-1} dr^2 + r^2 d\theta^2 + r^2 \sin^2\theta d\phi^2. \tag{3.1}$$

Here, the intruding object has the redshift function $\phi(r)$ defined in terms of radial coordinate r. The radial coordinate is specified as $0 < r_0 \leq r \leq \infty$ which clearly indicates its non-monotonic behavior, as we can gather from the above definition that r is dropped from ∞ to the minimum value r_0, which is also equal to $b(r_0)$, and again from r_0, the value approaches ∞. The smallest value of r is designated as the throat radius. The redshift function must have a finite value everywhere near the throat. Crucially, it cannot vanish, as this would lead to an event horizon or a singularity at the throat, thus compromising the wormhole's traversability. Our present study focuses on Casimir wormhole solutions that have a predetermined shape function $b(r)$ and redshift function [61]. The shape function must satisfy some constraints as it ascertains the wormhole geometry. The flaring out condition, $b'(r_0) < 1$, establishes traversability within the wormhole's space-time. This condition determines the minimum size of the throat, and therefore the validation of the flaring-out condition is must to maintain the geometry of the wormhole. The conditions $0 < 1 - \frac{b(r)}{r}$ and $b(r_0) = r_0$, where $r_0 \leq r \leq \infty$, are called the throat condition. Here, r_0, as described above, is the throat radius and has the minimum value of r. Another important requirement imposed on the shape function is

$$\frac{b(r)}{r} \to 0 \qquad \text{as} \qquad |r| \to \infty,$$

known as the asymptotically flatness condition. This condition indicates that at large distances from a region, the curvature of the space-time vanishes. The proper radial distance is expressed as $x(r) = \pm \int_{r_0}^{r} \frac{dr}{\sqrt{\frac{r-b(r)}{r}}}$ is a decreasing function descending from upper space $x = +\infty$ to the throat of the wormhole and then coming down to $x = -\infty$. This proper distance must be finite with respect to the radial coordinate, but this distance $x(r)$ must abide by the condition $r - r_0 \leq |x(r)|$ i.e., the radial coordinate distance is always less than or equal to the proper radial distance. The lower and the upper regions of a wormhole are represented by the negative and positive values of x, which are connected by the throat where $x = 0$.

Our analysis presumes an anisotropic matter fluid within the wormhole throat, with its stress-energy-momentum tensor given by

$$T_l^m = (\rho + p_t)\, u_l u^m + p_t \delta_l^m + (p_r - p_t)\, v_l v^m. \tag{3.2}$$

Where, the unit space-like vector along the radial coordinate is expressed by v_l while u_l gives the four velocity. Energy density, radial and tangential pressures are represented by ρ, p_r, p_t respectively. For the line element Eq. (3.1), the trace Q of the non-metricity tensor in $f(Q)$ gravity is given by:

$$Q = -\frac{2}{r^3}\left[r - b(r)\right]\left[2.r.\phi'(r) + 1\right]. \tag{3.3}$$

We solve Eq. (2.7), Eq. (3.1) and Eq. (3.2) to get the expressions for energy density (ρ), radial pressure (p_r) and tangential pressure (p_t) as

$$\rho = \left[\frac{1}{r^3}\left(2r\phi'(r)\left(r - b(r)\right) - b(r) - rb'(r) + r\right)\right] f_Q + \frac{2}{r^2}\left(r - b(r)\right) f_Q + \frac{f}{2}, \tag{3.4}$$

$$p_r = -\left[\frac{2}{r^3}\left(r - b(r)\right)\left(2r\phi'(r) + 1\right) - 1\right] f_Q - \frac{f}{2}, \tag{3.5}$$

$$\begin{aligned} p_t = -&\left[\frac{1}{r^3}\left(\left[1 + \left(r\phi'(r) + 3\right) r\phi'(r) + r^2\phi''(r)\right]\left[r - b(r)\right] - \frac{1}{2}\left[1 + r\phi'(r)\right]\left[rb'(r) - b(r)\right]\right)\right] \\ & f_Q - \frac{1}{r^2}\left[r - b(r)\right]\left[1 + r\phi'(r)\right] f_Q - \frac{f}{2}. \end{aligned} \tag{3.6}$$

We may analyze the different solutions for wormhole geometry by selecting the appropriate shape function $b(r)$ and redshift function $\phi(r)$. In our current paper, we use Casimir's shape function and the redshift function to identify the presence of negative energy within the wormhole geometry.

4 Energy Constraints

The requisite constraints, generally referred to as energy conditions, constructed from Raichaudhary equations, set out the temporal evolution of the time-like vector u^l and k_l, which gives the null geodesics as

$$\frac{d\theta}{d\tau} - \omega_{lm}\omega^{lm} + \sigma_{lm}\sigma^{lm} + \frac{1}{3}\theta^2 + R_{lm}u^l u_m = 0, \tag{4.1}$$

$$\frac{d\theta}{d\tau} - \omega_{lm}\omega^{lm} + \sigma_{lm}\sigma^{lm} + \frac{1}{2}\theta^2 + R_{lm}k^l k_m = 0, \tag{4.2}$$

where, k^l denotes the vector field, on the other hand, the shear or spatial tensor is given by $R_{lm}k^l k_m$ having $\sigma^2 = \sigma_{lm}\sigma^{lm} \geq 0$ and $\omega_{lm} \equiv 0$.

These are the conditions that provide information regarding the type of fluid found in the wormhole throat. These circumstances are often evaluated in terms of the radial and tangential pressures alongside the energy density. The stability, development, and existence of traversable wormholes are determined by whether the energy criteria are validated or violated. These energy conditions concur with the Raichaudhary conditions in the case of positive energy, i.e., attractive geometry, also for $\theta < 0$.

$$R_{lm}u^l u_m \geq 0, \tag{4.3}$$

$$R_{lm}k^l k_m \geq 0. \tag{4.4}$$

Here, we consider the energy conditions for anisotropic matter fluid. The null energy condition (NEC) is expressed using the energy density ρ, radial pressure p_r, and tangential pressure p_t as $\forall i, \rho(r) + p_i \geq 0$ or $T_{lm}k^l k^m \geq 0$ in tensor form, indicating that these principle pressures are non-negative. In GR, the traversability of the wormhole is related to a violation of NEC. To guarantee a non-negative energy density for a time-like vector, the weak energy condition (WEC) must hold, which means $\rho(r) \geq 0$ and $\forall i, \rho(r) + p_i \geq 0$ or $T_{lm}k^l k^m \geq 0$. The strong energy condition (SEC) $(T_{lm} - \frac{T}{2}g_{lm})k^l k^m \geq 0$ in tensor form or $T = -\rho(r) + \sum_j p_j$ and $\forall j, \rho(r) + p_j \geq 0, \rho(r) + \sum_j p_j \geq 0$ in principle pressures is related to the universe's inflation. The SEC must be violated to acknowledge this inflation. The dominant energy condition (DEC) is a constraint on the energy transmission, which restricts its limit to the light's speed. The mass of energy cannot flow at a speed greater than light. In tensor form DEC is given as $T_{lm}k^l k^m \geq 0$, where $T_{lm}k^l$ is not space-like or $\rho(r) \geq 0$ and $\forall i, \rho \pm p_i \geq 0$ in terms of principle pressures.

5 The Casimir Energy Wormhole Model

As we know, traversable WH require exotic matter to violate the null energy condition. Therefore, Garattini developed a model for such wormholes, known as Casimir wormholes, by incorporating an equation of state arising from the Casimir effect. In Casimir wormhole models, the concept of exotic matter is replaced by the Casimir energy density, which is an imagined substance with a negative energy density. Currently, the Casimir effect is the only known physical phenomenon that provides a naturally occurring negative energy density

$$\rho_0 = -\frac{hc\pi^2}{720d^4}. \tag{5.1}$$

The Casimir energy's stress energy tensor (SET) is

$$T_{\mu\nu} = \frac{hc\pi^2}{720d^4}\left[dia\left(-1, -3, 1, 1\right)\right]. \tag{5.2}$$

Here, d signifies the plate separation, characterized by being both traceless and having a null divergence. Because of the quantum attributes of Casimir energy, the semi-classical Einstein Field Equation (EFE) $G_{\mu\nu} = \kappa\left(T_{\mu\nu}\right)^{Ren}$ is induced in the place of EFE, where the renormalized quantum contribution of specific matter field such as electromagnetic field is described by $(T_{\mu\nu})^{Ren}$. The relation between the aforementioned stress-energy tensor (SET) and the spacetime metric is established by calculating the Casimir shape function and redshift function, which are shown below [62]

$$b(r) = \frac{2r_0}{3} + \frac{{r_0}^2}{3r}, \quad \phi(r) = \ln\left(\frac{3r}{3r+r_0}\right). \tag{5.3}$$

Above results are obtained by using the equation of state (EoS) $\omega = \frac{p_r}{\rho}$.

The Equation of State (EoS) is important in understanding wormhole geometry because it shows the underlying nature of the matter that supports the throat. The matter corresponding to the EoS value $-1 < \omega < -1/3$ asserts the quintessence dark energy, which ascertains the expansion of the universe. The quintessence dark energy covers the case $\omega = -1$ as well. $\omega < -1$ indicates the phantom fluid, which also acknowledges the accelerated expansion of the universe.

5.1 Power Law Form: $f(Q) = \alpha Q^2 + \beta$

Now we examine the WH solutions in the backdrop of the power law form of $f(Q)$ stated as $f(Q) = \alpha Q^2 + \beta$, where α and β are constants, powered by Casimir energy. Previously also this form has also been studied for the possible wormhole solutions [52]. This power-law form already accommodates radiation-dominated backgrounds and cold dark matter (CDM). In this scenario, we calculate the energy components by solving the field equations shown below

$$\rho = \frac{1}{6r^8}\left\{3\beta r^8 - 48\alpha r^5 + 4\alpha r^4(8r_0+9) + 64\alpha r^3{r_0}^2 - 32\alpha r^2{r_0}^2(r_0+2) - 16\alpha r{r_0}^4 + 28\alpha{r_0}^4\right\}, \tag{5.4}$$

$$p_r = -\frac{\beta}{2} + \frac{6\alpha{r_0}^4}{r^8} - \frac{8\alpha{r_0}^2}{r^6} + \frac{2\alpha}{r^4}, \tag{5.5}$$

$$\begin{aligned} p_t &= \frac{1}{6r^8(3r+r_0)}\left\{3r^9(8\alpha r_0 - 3\beta) + r^8 r_0(40\alpha r_0 - 3\beta) - 8\alpha r^7{r_0}^3 - 8\alpha r^6\left(5{r_0}^4 - 9\right)\right. \\ &- 4\alpha r^5\left(4{r_0}^5 - 9\right) - 4\alpha r^4 r_0(32r_0+3) - 8\alpha r^3{r_0}^2(2r_0+5) + 8\alpha r^2{r_0}^3(7r_0-1) \\ &+ \left. 4\alpha r{r_0}^4(4r_0+1) + 20\alpha{r_0}^5\right\}. \end{aligned} \tag{5.6}$$

For this case, all the energy conditions, energy density ρ, and the EoS parameter ω are coined for positive values of α and $\beta = -1$. The nature of energy density, as depicted in Fig. 1(a), comes out to be negative throughout the region for different values of α. From Fig. 1(b) and Fig. 2(a), it is clear that radial NEC is violated while tangential NEC is validated. Hence, we can say that overall NECs are violated, which confirms the presence of exotic matter near the wormhole throat. From Fig. 2(b), the SEC is also satisfied in the entire region for all values of α. Figure 3 depicts the dominant energy condition (DEC), with the radial component shown in Fig. 3(a) and the tangential component shown in Fig. 3(b); both are violated at each value of α. The anisotropy parameter (Fig. 4(b)) was found to be positive in the entire region, which shows the repulsive behavior of the geometry. The EoS parameter is generally negative for all investigated $\alpha = (0.5, 1, 1.5, 2)$ within the geometry, as shown in Fig. 4(a). Interestingly, the parameter is positive close to the throat for $\alpha = 1.5, 2$, but it turns negative as the throat radius increases. As we can see that $\omega > -1$ for $r \geq r_0$, which signifies the universe's accelerated expansion.

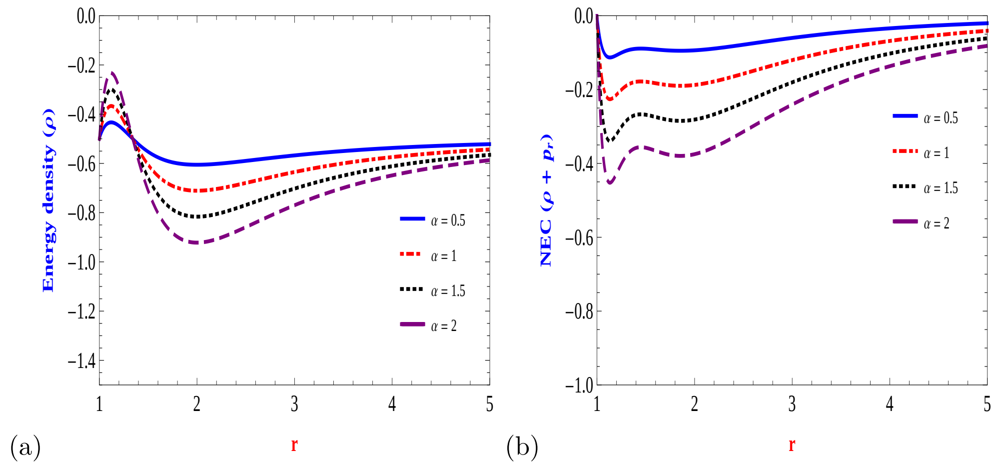

Figure 1: Plots of energy density (ρ) and radial null energy condition ($\rho + p_r$) for $\beta = -1$ and throat radius $r_0 = 1$.

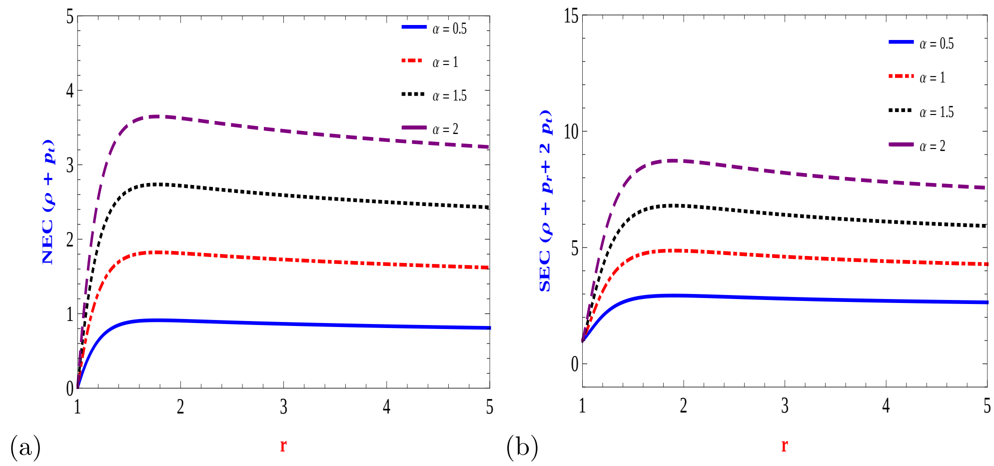

Figure 2: Plots of tangential null energy condition ($\rho + p_t$) and strong energy condition ($\rho + p_r + 2p_t$) for $\beta = -1$ and throat radius $r_0 = 1$.

5.2 Inverse Power Law form: $f(Q) = \alpha Q + \frac{\beta}{Q}$

This section presents the results obtained from the inverse power law form of teleparallel gravity (as explained in [63]) in the context of Casimir energy. The stress-energy tensor profile, encompassing the energy density ρ, radial pressure p_r, and tangential pressure p_t, is derived from equations (3.4), (3.5), and (3.6) as follows:

$$\begin{aligned}\rho &= \frac{1}{12r^4(r-r_0)^2(r+r_0)^2}\left[-6\beta r^{11} + 4\beta r^{10} r_0 + 2\beta r^9 r_0^2 + \beta r^8 r_0^2 + 24\alpha r^7\right.\\ &- 8\alpha r^6(2r_0+3) - 56\alpha r^5 r_0^2 + 4\alpha r^4 r_0^2(8r_0+17) + 40\alpha r^3 r_0^4 - 16\alpha r^2 r_0^4(r_0+4)\\ &- \left. 8\alpha r r_0^6 + 20\alpha r_0^6\right], \end{aligned} \tag{5.7}$$

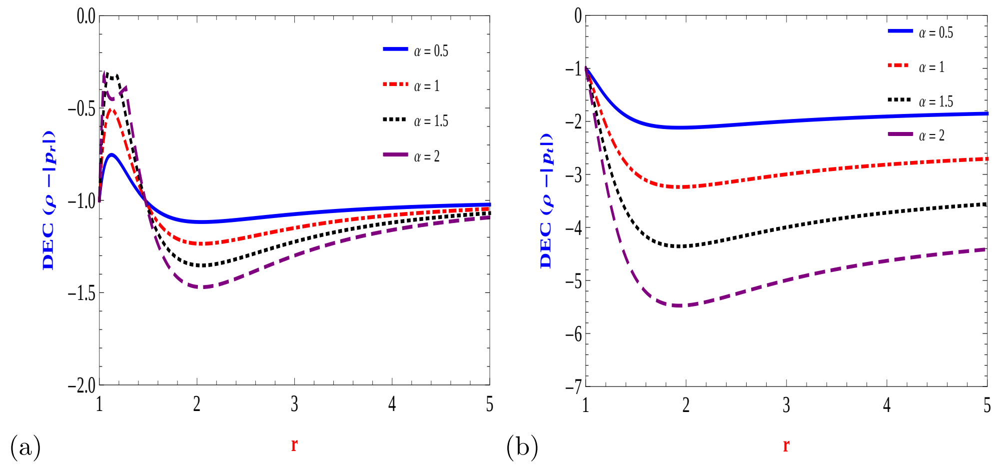

Figure 3: Plots of radial and tangential DECs ($\rho - |p_r|$, $\rho - |p_t|$) for $\beta = -1$ and throat radius $r_0 = 1$.

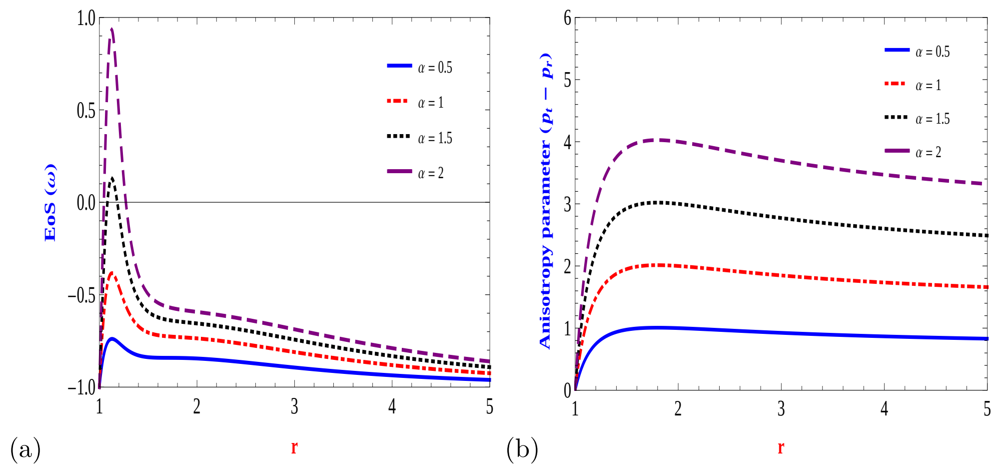

Figure 4: Plots of EoS parameter (ω) and Anisotropic parameter ($p_t - p_r$) for $\beta = -1$ and throat radius $r_0 = 1$

$$p_r = \frac{1}{4r^4(r-r_0)^2(r+r_0)^2}\left[2\beta r^{10} - 3\beta r^8 r_0^2 + 4\alpha r^4 r_0^2 - 8\alpha r^2 r_0^4 + 4\alpha r_0^6\right], \tag{5.8}$$

$$\begin{aligned} p_t \;&=\; \frac{1}{12r^4(r-r_0)^2(r+r_0)^2(3r+r_0)}\left[3\beta r^{15} r_0 + 5\beta r^{14} {r_0}^2 + 2\beta r^1 3{r_0}^3\right. \\ &+\; 9\beta r^{12} - 6r^{11}(2\alpha r_0 - 3\beta) + r^{10} r_0(3\beta - 20\alpha r_0 - 7\beta r_0) + 2r^9 r_0^2(-7\beta \\ &+\; 8\alpha r_0 - \beta r_0) + r^8\left(4\alpha\left(10r_0^4 - 9\right) - 7\beta r_0^3\right) + 4\alpha r^7 r_0^5 - 4\alpha r^6 r_0\left(5r_0^5 - 25r_0 - 3\right) \\ &-\; 8\alpha r^5 r_0^2\left(r_0^5 - r_0 + 2\right) - 4\alpha r^4 r_0^3(23r_0 + 5) - 16\alpha r^3(r_0 - 2)r_0^4 + 4\alpha r^2 r_0^5(7r_0 + 1) \\ &+\; \left. 8\alpha r(r_0 - 2)r_0^6 + 4\alpha r_0^7\right]. \end{aligned} \tag{5.9}$$

The several energy conditions, EoS parameter, and anisotropy parameter are formulated in Fig. (5)-Fig. (8). The plots are taken against $\alpha = 0.2$ and $\beta = (0.05, 0.06, 0.07, 0.08)$. As one can see from Fig. 5(a), for positive values of β, the energy density is initially positive at the throat but tends to negative when r and β increase. From Figs. 5(b) and 6(a), it is clear that the NECs are violated. This is an indication of the existence of negative energy. The wormhole spacetime geometry is shown to be repulsive, as evidenced by consistently positive values of the anisotropy parameter (Fig. 8(a)) for all β occurrences. The violation of energy conditions shows that there is exotic energy within the throat of the wormhole geometry, which we can suggest to be the effect of the Casimir system. The Casimir energy can be assumed to source this exotic energy to sustain the wormhole.

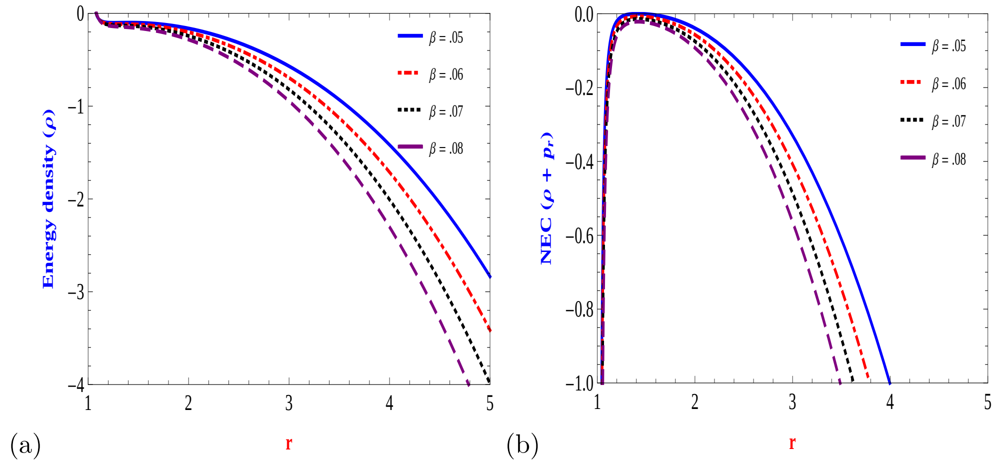

Figure 5: Plots of energy density (ρ) and radial null energy condition ($\rho + p_r$) for $\alpha = 0.2$ and throat radius $r_0 = 1$.

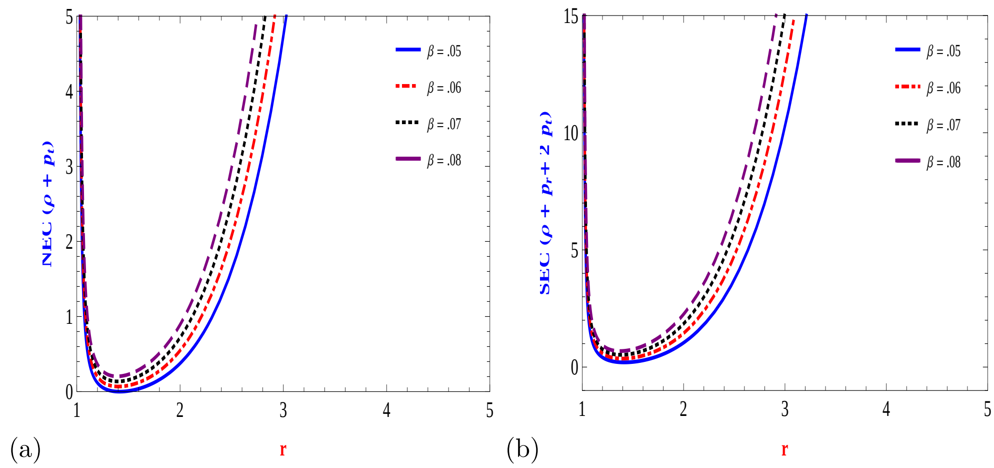

Figure 6: Plots of tangential null energy condition ($\rho + p_t$) and strong energy condition ($\rho + p_r + 2p_t$) for $\alpha = 0.2$ and throat radius $r_0 = 1$.

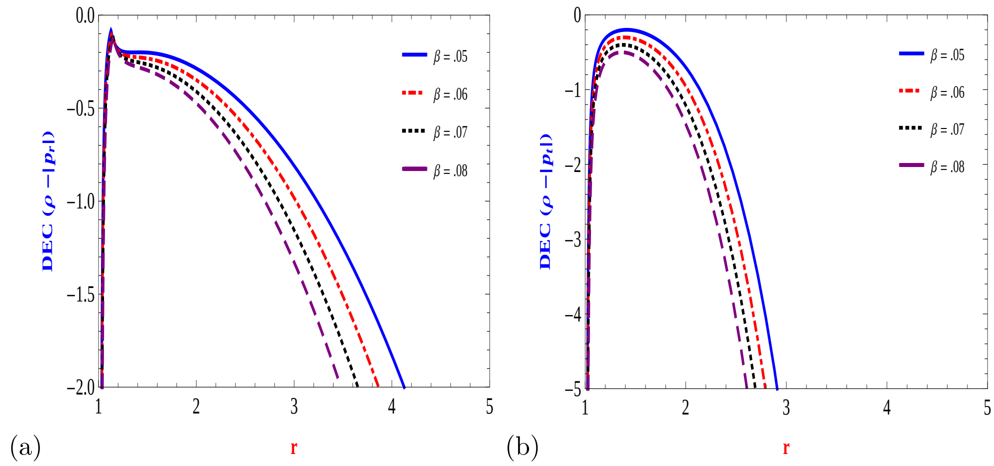

Figure 7: Plots of radial and tangential DECs ($\rho - |p_r|$, $\rho - |p_t|$) for $\alpha = 0.2$ and throat radius $r_0 = 1$.

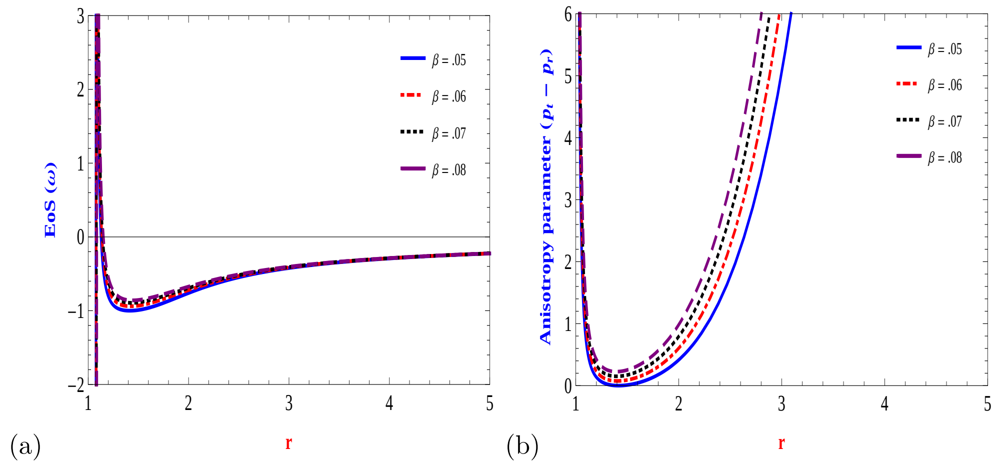

Figure 8: Plots of EoS parameter (ω) and Anisotropic parameter ($p_t - p_r$) for $\alpha = 0.2$ and throat radius $r_0 = 1$.

5.3 Logarithmic form: $f(Q) = Q + \alpha \log(\beta Q)$

In the last case, we consider the logarithmic form of the function $f(Q)$ such that $f(Q) = Q + \alpha \log(\beta Q)$, where α and β are constants. Mathematically stated, logarithmic functions form provides equations allowing the existence of traversable and stable wormhole solutions. A need for exotic matter can be diminished or even eliminated entirely by using the logarithmic form of f(Q) gravity. We incorporate the abovementioned specific shape function $b(r)$ and redshift function $\phi(r)$ corresponding to Casimir energy (Eq. (5.3)) in the Eqs. (3.4), (3.5) and (3.6), The energy density and principal pressures were obtained as functions of the radial coordinate r, as

$$\begin{aligned}\rho &= \frac{1}{6r^4(r-r_0)(r+r_0)}\left[-6\alpha r^7+\alpha r^6(4r_0+3)+2r^5\left(\alpha r_0^2+6\right)-2r^4\left(\alpha r_0^2+4r_0+6\right)\right.\\ &- 16r^3r_0^2+2r^2r_0^2(4r_0+11)+3\alpha r^4\left(r^2-r_0^2\right)\log\left(-\frac{2\beta(r-r_0)(r+r_0)}{r^4}\right)\\ &+ \left. 4rr_0^4-10r_0^4\right],\end{aligned} \tag{5.10}$$

$$\begin{aligned}p_r &= \frac{1}{2r^4(r-r_0)(r+r_0)}\left[\alpha r^6-2\alpha r^4r_0^2+2r^2r_0^2+\alpha r^4\left(r_0^2-r^2\right)\log\left(-\frac{2\beta(r-r_0)(r+r_0)}{r^4}\right)\right.\\ &- \left. 2r_0^4\right],\end{aligned} \tag{5.11}$$

$$\begin{aligned}p_t &= \frac{1}{6r^4(r-r_0)(r+r_0)(3r+r_0)}\left[\alpha r^{11}r_0+5\alpha r^{10}r_0^2+2r^9r_0\left(\alpha r_0^2-3\right)+r^8\left(9\alpha-10r_0^2\right)\right.\\ &+ r^7\left(9\alpha+2r_0^3\right)+r^6\left(10r_0^4-7\alpha r_0^2-18\right)+r^5r_0^2\left(-5\alpha+4r_0^3-2\alpha r_0\right)\\ &+ 2r^4r_0\left(-2\alpha r_0^2+16r_0+3\right)+4r^3(r_0-2)r_0^2-2r^2r_0^3(7r_0+2)\\ &+ 3\alpha r^4\left(-3r^3-r^2r_0+3rr_0^2+r_0^3\right)\log\left(-\frac{2\beta(r-r_0)(r+r_0)}{r^4}\right)\\ &- \left. 4r(r_0-2)r_0^4-2r_0^5\right].\end{aligned} \tag{5.12}$$

These principle pressures in the form of energy constraints, as discussed section 4, along with the EoS parameter on variation of radial coordinate r and different values of α and $\beta=-100$ are plotted in Fig. 9 to Fig. 12 to study the wormhole conformation. We now go ahead to investigate the implications of the plots to investigate the possible Casimir WH solution. The energy density ρ for this logarithmic case is plotted in Fig. 9(a) for different values of $\alpha=(1,1.5,2,2.5)$ and $\beta=-100$. The energy density is consistently found to be negative for all values of α and for $r\geq r_0$. The energy density is found to be negative everywhere for all values of α and for $r\geq r_0$. From Figs. 9(b) and 10(a), it can be gathered that the NEC is violated as the NEC corresponding to the tangential pressure is validated while the radial NEC is not satisfied throughout the region $r\geq r_0$. This violation of the null energy condition (NEC) signifies the presence of exotic matter near the throat, which is essential for supporting the wormhole's geometry. Figures 10(b), 11(a), and 11(b) show the SEC and DEC, both of which are violated. The EoS and anisotropic parameter are plotted in Figs. 12(a) and 12(b). A positive anisotropic parameter value indicates that the geometry is repulsive in nature.

6 Conclusions

In GR the existence of WH geometry is associated with an unavoidable repercussion of GR, which is the violation of NECs leading to the existence of non-ordinary matter in the WH throat. Although in recent times, researchers are more concerned about finding the WH geometry filled with classical matter or minimizing the presence of exotic matter using the framework of modified theories of gravity. In our present study, we aim to find the Casimir energy effect in wormhole geometry. We examined static, spherically symmetric wormholes in the context of symmetric teleparallel gravity. In this model, the non-metricity term Q

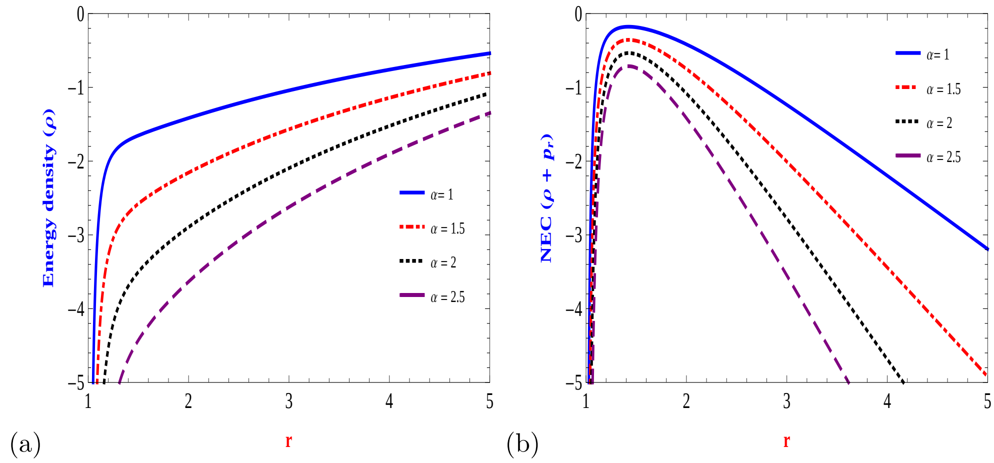

Figure 9: Plots of energy density (ρ) and radial null energy condition $(\rho + p_r)$ for $\beta = -100$ and throat radius $r_0 = 1$.

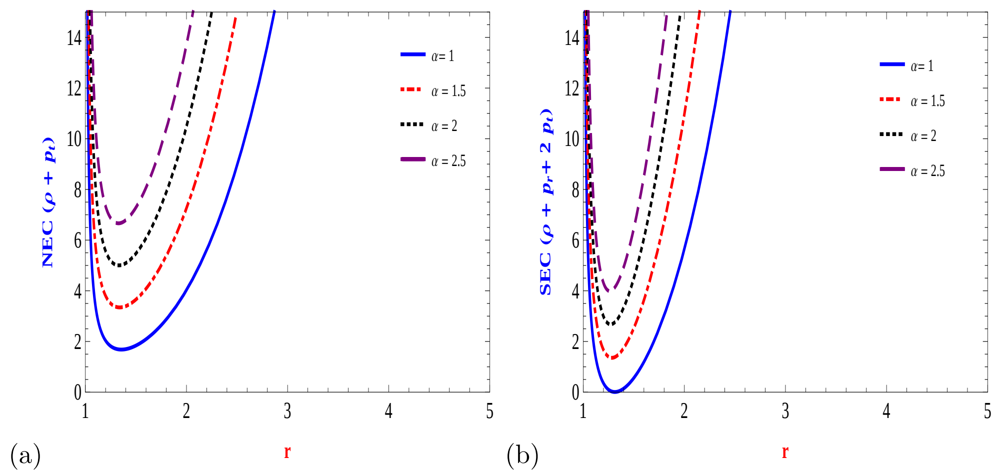

Figure 10: Plots of tangential null energy condition $(\rho + p_t)$ and strong energy condition $(\rho + p_r + 2p_t)$ for $\beta = -100$ and throat radius $r_0 = 1$.

defines spacetime's gravitational interactions, which include Casimir energy. We investigated traversable wormhole solutions created by the Casimir apparatus, exploring them within all three functional forms of $f(Q)$ gravity. We discovered that Casimir energy serves as a source of exotic (negative) energy capable of maintaining the traversability of wormhole geometry. We also attempted to create a wormhole geometry in which the negative energy required is derived directly from Casimir energy, rather than relying on hypothetical exotic materials. So, we can also think about traversable wormholes, which are self-sustained, i.e., they are sustained by their own quantum fluctuations [64–67]. It will be interesting to see how the Casimir energy and quantum fluctuations carried by the gravitons interact if TW can be self-sustained. In this scenario, the Casimir source could be understood as the switch that turns on the wormhole's traversability.

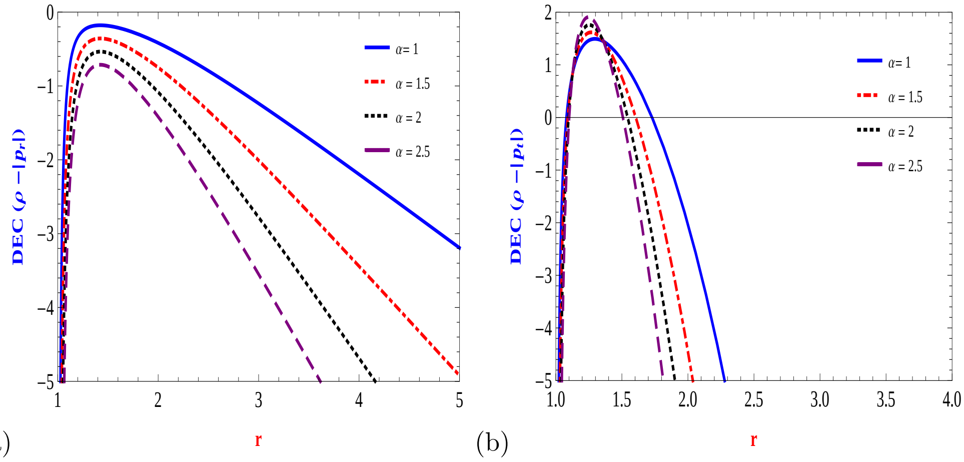

Figure 11: Plots of radial and tangential DECs ($\rho - |p_r|$, $\rho - |p_t|$) for $\beta = -100$ and throat radius $r_0 = 1$.

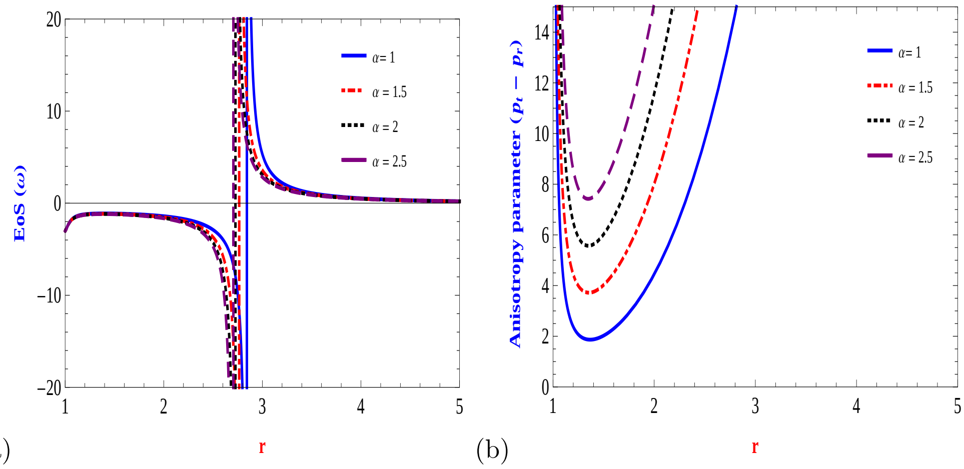

Figure 12: Plots of EoS parameter (ω) and Anisotropic parameter ($p_t - p_r$) for $\beta = -100$ and throat radius $r_0 = 1$.

Authors' Contributions

All authors have the same contribution.

Data Availability

The manuscript has no associated data or the data will not be deposited.

Conflicts of Interest

The author declares that there is no conflict of interest.

Ethical Considerations

The author has diligently addressed ethical concerns, such as informed consent, plagiarism, data fabrication, misconduct, falsification, double publication, redundancy, submission, and other related matters.

Funding

This research was supported by the Russian Science Foundation through a grant to the Laboratory of Solar Astronomy at the Space Research Institute of the Russian Academy of Sciences.

Acknowledgements

The authors would like to thank the learned reviewer(s) for their elaborate and valuable comments and suggestions that help us to improve this paper significantly in the present form.

References

[1] K. Akiyama *et al.* [Event Horizon Telescope], “First M87 Event Horizon Telescope Results. VIII. Magnetic Field Structure near The Event Horizon,” Astrophys. J. Lett. **910**(1), L13 (2021). DOI:10.3847/2041-8213/abe4de

[2] L. Blackburn *et al.* “Studying Black Holes on Horizon Scales with VLBI Ground Arrays,” (2019). [arXiv:1909.01411 [astro-ph.IM]].

[3] R. Abuter *et al.* [GRAVITY], “Detection of the Schwarzschild precession in the orbit of the star S2 near the Galactic centre massive black hole,” Astron. Astrophys. **636** L5 (2020). DOI:10.1051/0004-6361/202037813

[4] E. Gourgoulhon, A. Le Tiec, F. H. Vincent and N. Warburton, “Gravitational waves from bodies orbiting the Galactic Center black hole and their detectability by LISA,” Astron. Astrophys. **627** A92 (2019). DOI:10.1051/0004-6361/201935406

[5] B. P. Abbott *et al.* [LIGO Scientific and Virgo], “Observation of Gravitational Waves from a Binary Black Hole Merger,” Phys. Rev. Lett. **116** no.6, 061102 (2016). DOI:10.1103/PhysRevLett.116.061102

[6] L. Flamm, “Comments on Einstein’s theory of gravity,” Phys. Z. **17** 448 (1916).

[7] S. Capozziello and M. De Laurentis, “Extended Theories of Gravity,” Phys. Rept. **509** 167-321 (2011). DOI:10.1016/j.physrep.2011.09.003

[8] A. Einstein and N. Rosen, “The Particle Problem in the General Theory of Relativity,” Phys. Rev. **48** 73-77 (1935). DOI:10.1103/PhysRev.48.73

[9] K. Jusufi and A. Övgün, “Gravitational Lensing by Rotating Wormholes,” Phys. Rev. D **97** no.2, 024042 (2018). DOI:10.1103/PhysRevD.97.024042

[10] A. Övgün, K. Jusufi and İ. Sakallı, "Exact traversable wormhole solution in bumblebee gravity," Phys. Rev. D **99** no.2, 024042 (2019). DOI:10.1103/PhysRevD.99.024042

[11] M. S. Morris and K. S. Thorne, "Wormholes in space-time and their use for interstellar travel: A tool for teaching general relativity," Am. J. Phys. **56** 395-412 (1988). DOI:10.1119/1.15620

[12] M. S. Morris, K. S. Thorne and U. Yurtsever, "Wormholes, Time Machines, and the Weak Energy Condition," Phys. Rev. Lett. **61** 1446-1449 (1988). DOI:10.1103/PhysRevLett.61.1446

[13] G. Clement, "The Ellis geometry," Am. J. Phys. **57**(11), 967 (1989).

[14] H. a. Shinkai and S. A. Hayward, "Fate of the first traversible wormhole: Black hole collapse or inflationary expansion," Phys. Rev. D **66**, 044005 (2002). DOI:10.1103/PhysRevD.66.044005

[15] S. W. Kim and K. S. Thorne, "Do vacuum fluctuations prevent the creation of closed timelike curves?," Phys. Rev. D **43**, 3929 (1991). DOI:10.1103/PhysRevD.43.3929

[16] M. Visser, "Lorentzian Wormholes: From Einstein to Hawking," American Institute of Physics, New York (1995).

[17] K. Jusufi, A. Banerjee and S. G. Ghosh, "Wormholes in 4D Einstein–Gauss–Bonnet gravity," Eur. Phys. J. C **80**(8), 698 (2020). DOI:10.1140/epjc/s10052-020-8287-x

[18] S. V. Sushkov, "Wormholes supported by a phantom energy," Phys. Rev. D **71**, 043520 (2005). DOI:10.1103/PhysRevD.71.043520

[19] D. Wang and X. H. Meng, "Wormholes supported by phantom energy from Shan–Chen cosmological fluids," Eur. Phys. J. C **76**(3), 171 (2016). DOI:10.1140/epjc/s10052-016-4024-x

[20] P. K. Sahoo, P. H. R. S. Moraes, P. Sahoo and G. Ribeiro, "Phantom fluid supporting traversable wormholes in alternative gravity with extra material terms," Int. J. Mod. Phys. D **27**(16), 1950004 (2018). DOI:10.1142/S0218271819500044

[21] F. S. N. Lobo, "Phantom energy traversable wormholes," Phys. Rev. D **71**, 084011 (2005). DOI:10.1103/PhysRevD.71.084011

[22] Shweta, A. K. Mishra and U. K. Sharma, "Traversable wormhole modelling with exponential and hyperbolic shape functions in $F(R,T)$ framework," Int. J. Mod. Phys. A **35**(25), 2050149 (2020). DOI:10.1142/S0217751X20501493

[23] P. H. R. S. Moraes and P. K. Sahoo, "Modelling wormholes in $f(R,T)$ gravity," Phys. Rev. D **96**(4), 044038 (2017). DOI:10.1103/PhysRevD.96.044038

[24] P. K. Sahoo, P. H. R. S. Moraes and P. Sahoo, "Wormholes in R^2 -gravity within the f(R, T) formalism," Eur. Phys. J. C **78**(1), 46 (2018). DOI:10.1140/epjc/s10052-018-5538-1

[25] M. Zubair, S. Waheed, G. Mustafa and H. Ur Rehman, "Noncommutative inspired wormholes admitting conformal motion involving minimal coupling," Int. J. Mod. Phys. D **28**(04), 1950067 (2019). DOI:10.1142/S0218271819500676

[26] U. K. Sharma and A. K. Mishra, "Wormholes Within the Framework of $f(R,T) = R+\alpha R^2+\lambda T$ Gravity," Found. Phys. **51**(2), 50 (2021). DOI:10.1007/s10701-021-00457-6

[27] A. K. Mishra and U. K. Sharma, “Wormhole models in R^2-gravity for $f(R,T)$ theory with a hybrid shape function,” Can. J. Phys. **99**(6), 481 (2021). DOI:10.1139/cjp-2020-0485

[28] G. Mustafa, X. Tie-Cheng, M. Ahmad and M. F. Shamir, “Anisotropic spheres via embedding approach in R+βR2 gravity with matter coupling,” Phys. Dark Univ. **31**, 100747 (2021). DOI:10.1016/j.dark.2020.100747

[29] P. H. R. S. Moraes and P. K. Sahoo, “Wormholes in exponential $f(R,T)$ gravity,” Eur. Phys. J. C **79**(8), 677 (2019). DOI:10.1140/epjc/s10052-019-7206-5

[30] S. Capozziello, T. Harko, T. S. Koivisto, F. S. N. Lobo and G. J. Olmo, “Wormholes supported by hybrid metric-Palatini gravity,” Phys. Rev. D **86**, 127504 (2012). DOI:10.1103/PhysRevD.86.127504

[31] A. Dixit, C. Chawla and A. Pradhan, “Traversable wormholes with logarithmic shape function in f(R, T) gravity,” Int. J. Geom. Meth. Mod. Phys. **18**(04), 2150064 (2021). DOI:10.1142/S021988782150064X

[32] N. Godani and G. C. Samanta, “Charged traversable wormholes in $f(R)$ gravity,” Int. J. Geom. Meth. Mod. Phys. **18**(07), 2150098 (2021). DOI:10.1142/S0219887821500985

[33] N. Godani, “Wormhole solutions in f(R,T) gravity,” New Astron. **94**, 101774 (2022). DOI:10.1016/j.newast.2022.101774

[34] N. Godani, “Thin-shell wormholes in non-linear f(R) gravity with variable scalar curvature,” New Astron. **96**, 101835 (2022). DOI:10.1016/j.newast.2022.101835

[35] N. Godani, D. V. Singh and G. C. Samanta, “Stability of thin-shell wormhole in 4D Einstein–Gauss–Bonnet gravity,” Phys. Dark Univ. **35**, 100952 (2022). DOI:10.1016/j.dark.2022.100952

[36] Y. Feng, “Gaussian and Lorentzian non-commutative wormhole solutions in exponential gravity,” New Astron. **97**, 101858 (2022). DOI:10.1016/j.newast.2022.101858

[37] A. K. Mishra and U. K. Sharma, “A new shape function for wormholes in $f(R)$ gravity and General Relativity,” New Astron. **88**, 101628 (2021). DOI:10.1016/j.newast.2021.101628

[38] V. De Falco, E. Battista, S. Capozziello and M. De Laurentis, “Reconstructing wormhole solutions in curvature based Extended Theories of Gravity,” Eur. Phys. J. C **81**(2), 157 (2021). DOI:10.1140/epjc/s10052-021-08958-4

[39] G. Mustafa, M. Ahmad, A. Övgün, M. F. Shamir and I. Hussain, “Traversable Wormholes in the Extended Teleparallel Theory of Gravity with Matter Coupling,” Fortsch. Phys. **69**(8-9), 2100048 (2021). DOI:10.1002/prop.202100048

[40] K. N. Singh, A. Banerjee, F. Rahaman and M. K. Jasim, “Conformally symmetric traversable wormholes in modified teleparallel gravity,” Phys. Rev. D **101**(8), 084012 (2020). DOI:10.1103/PhysRevD.101.084012

[41] C. G. Boehmer, T. Harko and F. S. N. Lobo, “Wormhole geometries in modified teleparralel gravity and the energy conditions,” Phys. Rev. D **85**, 044033 (2012). DOI:10.1103/PhysRevD.85.044033

[42] R. Aldrovandi, J. G. Pereira, "Teleparallel Gravity: An Introduction," Fundam.Theor.Phys. **173**, (2013). DOI:10.1007/978-94-007-5143-9.

[43] J. Beltrán Jiménez, L. Heisenberg, T. Koivisto, "Coincident General Relativity," Phys. Rev. D **98**(4), 044048 (2018). DOI.org/10.1103/PhysRevD.98.044048.

[44] R. Lazkoz, F. S. N. Lobo, M. Ortiz-Baños and V. Salzano, "Observational constraints of $f(Q)$ gravity," Phys. Rev. D **100**(10), 104027 (2019). DOI:10.1103/PhysRevD.100.104027

[45] I. Ayuso, R. Lazkoz and V. Salzano, "Observational constraints on cosmological solutions of $f(Q)$ theories," Phys. Rev. D **103**(6), 063505 (2021). DOI:10.1103/PhysRevD.103.063505

[46] V. C. de Andrade, L. C. T. Guillen and J. G. Pereira, "Gravitational energy momentum density in teleparallel gravity," Phys. Rev. Lett. **84**, 4533 (2000). DOI:10.1103/PhysRevLett.84.4533

[47] S. Mandal, P. K. Sahoo and J. R. L. Santos, "Energy conditions in $f(Q)$ gravity," Phys. Rev. D **102**(2), 024057 (2020). DOI:10.1103/PhysRevD.102.024057

[48] S. Mandal, D. Wang and P. K. Sahoo, "Cosmography in $f(Q)$ gravity," Phys. Rev. D **102**, 124029 (2020). DOI:10.1103/PhysRevD.102.124029

[49] T. Harko, T. S. Koivisto, F. S. N. Lobo, G. J. Olmo and D. Rubiera-Garcia, "Coupling matter in modified Q gravity," Phys. Rev. D **98**(8), 084043 (2018). DOI:10.1103/PhysRevD.98.084043

[50] Z. Hassan, S. Mandal and P. K. Sahoo, "Traversable Wormhole Geometries in Gravity," Fortsch. Phys. **69**(6), 2100023 (2021). DOI:10.1002/prop.202100023

[51] Z. Hassan, G. Mustafa and P. K. Sahoo, "Wormhole Solutions in Symmetric Teleparallel Gravity with Noncommutative Geometry," Symmetry **13**(7), 1260 (2021). DOI:10.3390/sym13071260

[52] U. K. Sharma, Shweta and A. K. Mishra, "Traversable wormhole solutions with non-exotic fluid in framework of f(Q) gravity," Int. J. Geom. Meth. Mod. Phys. **19**(02), 2250019(2022). DOI:10.1142/S0219887822500190

[53] J. W. Maluf, "The teleparallel equivalent of general relativity," Annalen Phys. **525**, 339 (2013). DOI:10.1002/andp.201200272

[54] G. Plunien, B. Muller and W. Greiner, "The Casimir Effect," Phys. Rept. **134**, 87 (1986). DOI:10.1016/0370-1573(86)90020-7

[55] M. Sparnaay, "Attractive forces between flat plates," Nature **180**, 334 (1957). DOI:https://doi.org/10.1038/180334b0

[56] M. Sparnaay, "Measurement of attractive forces between flat plates," Physica **24**, 751 (1958). DOI.org/10.1016/S0031-8914(58)80090-7.

[57] S. K. Lamoreaux, "Demonstration of the Casimir force in the 0.6 to 6 micrometers range," Phys. Rev. Lett. **78**, 5 (1997). [Erratum: Phys. Rev. Lett. **81** 5475-5476 (1998)]. DOI:10.1103/PhysRevLett.78.5

[58] G. Bressi, G. Carugno, R. Onofrio and G. Ruoso, "Measurement of the Casimir force between parallel metallic surfaces," Phys. Rev. Lett. **88**, 041804 (2002). DOI:10.1103/PhysRevLett.88.041804

[59] J. Beltrán Jiménez, L. Heisenberg, T. S. Koivisto and S. Pekar, "Cosmology in $f(Q)$ geometry," Phys. Rev. D **101**(10), 103507 (2020). DOI:10.1103/PhysRevD.101.103507

[60] P. H. F. Oliveira, G. Alencar, I. C. Jardim and R. R. Landim, "Traversable Casimir wormholes in D dimensions," Mod. Phys. Lett. A **37**(15), 2250090 (2022). DOI:10.1142/S0217732322500900

[61] R. Garattini, "Generalized Absurdly Benign Traversable Wormholes powered by Casimir Energy," Eur. Phys. J. C **80**(12), 1172 (2020). DOI:10.1140/epjc/s10052-020-08728-8

[62] R. Garattini, "Casimir Wormholes," Eur. Phys. J. C **79**(11), 951 (2019). DOI:10.1140/epjc/s10052-019-7468-y

[63] A. Banerjee, A. Pradhan, T. Tangphati and F. Rahaman, "Wormhole geometries in $f(Q)$ gravity and the energy conditions," Eur. Phys. J. C **81**(11), 1031 (2021). DOI:10.1140/epjc/s10052-021-09854-7

[64] R. Garattini, "Self sustained traversable wormholes?," Class. Quant. Grav. **22**, 1105 (2005). DOI:10.1088/0264-9381/22/6/012

[65] R. Garattini and F. S. N. Lobo, "Self sustained phantom wormholes in semi-classical gravity," Class. Quant. Grav. **24**, 2401 (2007). DOI:10.1088/0264-9381/24/9/016

[66] R. Garattini and F. S. N. Lobo, "Self-sustained traversable wormholes in noncommutative geometry," Phys. Lett. B **671**, 146 (2009). DOI:https://doi.org/10.1016/j.physletb.2008.11.064

[67] R. Garattini and F. S. N. Lobo, "Self-sustained wormholes in modified dispersion relations," Phys. Rev. D **85**, 024043 (2012). DOI:10.1103/PhysRevD.85.024043